EuroIntervention

Tissue characterisation of atherosclerotic plaque in coronary artery bifurcations: an intravascular ultrasound radiofrequency data analysis in humans

Seung Hwan Han[1,7], MD; Joseph Puma[2], MD; Hector M. Garcia-Garcia[3], MD, PhD; Kenya Nasu[4], MD; Pauliina Margolis[5], MD, PhD; Martin B. Leon[6], MD; Amir Lerman[7]*, MD

1. Division of Cardiology, Gil Hospital, Gachon University of Medicine and Science, Incheon, South Korea; 2. Division of Cardiology, Lenox Hill Heart & Vascular Institute, New York, NY, USA; 3. Thoraxcenter, Erasmus Medical Center, Rotterdam, The Netherlands; 4. Department of Cardiology, Toyohashi Heart Center, Aichi, Japan; 5. Volcano Corporation, Rancho Cordova, CA, USA; 6. Cardiovascular Research Foundation, New York, NY, USA; 7. Division of Cardiovascular Diseases and the Center for Coronary Physiology and Imaging, Mayo Clinic, MN, USA

MP Margolis is Medical Director of Volcano Corporation, Rancho Cordova, CA. MB Leon is a consultant and serves on the scientific advisory board of Volcano. The other authors have no conflict of interest to declare.

KEYWORDS
Atherosclerosis, bifurcation, intracoronary ultrasound, virtual histology

Abstract

Aims: To investigate tissue characteristics of atherosclerotic plaques in coronary artery bifurcations.

Methods and results: Using a global virtual histology registry, geometric and compositional characteristics of plaque in three segments (proximal, distal, and at the bifurcation) of coronary bifurcation sites were analysed with intravascular ultrasound radiofrequency data (RFD) analysis. A total of 256 bifurcation sites were analysed: left main (LM)-left anterior descending artery (LAD), 41; LAD-diagonal artery, 128; left circumflex artery-obtuse marginal artery, 34; and right coronary artery-acute marginal artery, 53. The plaque+media (P+M) burden was larger in the distal segments of LM-LAD bifurcation sites than in the proximal and at the bifurcation segments (46.55±12.08% vs. 40.40±11.76%, 41.15±11.01%, p<0.001). The % necrotic core (NC) and % dense calcium (DC) at the bifurcation and distal segments of LM-LAD bifurcation sites was significantly greater than in the proximal segments (6.75±5.09%, 7.36±6.01% vs. 4.89±4.78%, p<0.05, and 3.31±2.87%, 3.73±3.28% vs. 1.89±2.10%, p<0.001). In contrast, P+M burden, % NC and % DC in the proximal segments of non-LM bifurcation sites was significantly greater than at the bifurcation and distal segments (49.41±12.12% vs. 45.34±11.21%, 46.80±10.68% / 8.08±6.21% vs. 6.47±5.11%, 6.28±5.05% / 4.57±4.67% vs. 3.38±3.44%, 3.55±3.74%, all p<0.001).

Conclusions: The results demonstrate that heterogeneous nature of coronary atherosclerosis at coronary bifurcations according to their segments and anatomical locations (LM-LAD vs. non-LM bifurcations). The further investigation for the clinical efficacy of the RFD analysis on bifurcation sites are warranted.

** Corresponding author: Center for Coronary Physiology and Imaging, Mayo Clinic, 200 First Street SW, Rochester, MN 55905, USA*
E-mail: Lerman.amir@mayo.edu

Abbreviations

AM: acute marginal artery
CSA: cross-sectional area
IVUS: intravascular ultrasound
LAD: left anterior descending artery
LCX: left circumflex artery
LM: left main coronary artery
OM: obtuse marginal artery
P+M: plaque plus media
RCA: right coronary artery
RFD: radiofrequency data
VH: virtual histology (spectral analysis plaque characterisation methodology)

Introduction

Atherosclerotic plaques are prone to develop at specific locations such as coronary artery bifurcations and ostial locations.[1,2] Percutaneous coronary intervention of bifurcation lesions still remain a challenging lesion subset.[3] The distinctive lesion characteristics and adaptive arterial remodelling at bifurcation sites may occur because of geometric variation and additional factors such as shear stress, and vessel structure.[4-6]

The ability to visualise and quantify the different components of atherosclerosis provides important information not only on the mechanism of coronary artery disease, but also on potential future therapeutic interventions to alter the disease process and optimise interventional outcome. A new spectral analysis of the intravascular ultrasound (IVUS) radiofrequency data (RFD) may be a useful tool[7,8] because it allows detailed assessment of plaque composition, with a high predictive accuracy of 93.1% to 96.7% in fibrous tissue, fibro-fatty, dense calcium, and necrotic core regions with sensitivities and specificities ranging from 72% to 99%.[9] In addition, recent studies have demonstrated that IVUS RFD can discern tissue characteristics of patients with coronary artery disease in-vivo, and this imaging tool is useful in understanding the pathophysiology of the disease process.[10-12]

The compositional characteristics of coronary bifurcations have not been evaluated on the basis of their locations. Thus, the current study was designed to evaluate the geometric and compositional characteristics of atherosclerotic plaques in the proximal, distal and at the bifurcation segments of coronary bifurcation sites and to describe the distinguishing characteristics of atherosclerotic plaques in relation to their anatomic locations.

Methods

Study subjects

To evaluate the compositional characteristics of atherosclerotic plaque in coronary atherosclerosis, subjects who underwent IVUS-RFD analysis, virtual histology (VH) were prospectively enrolled in a multicenter, international, global VH registry. This protocol was approved by the local ethics committee. Written informed consent was obtained from every patient. For this study, we analysed the IVUS-RFD of major bifurcation sites (the diameter of side branch was more than 1.5 mm by IVUS) from this registry. The exclusion criteria of the present study were the presence of another intervening major side branch and the previous history of percutaneous coronary intervention within 10 mm of the index bifurcation sites. Non-native coronary artery, the sites with inadequate length of bifurcation segments for data analysis, the study which performed in saphenous vein graft, diagonal branch, obtuse marginal branch, poor image quality for the data analysis were further excluded.

IVUS-RFD examination

The methods of the IVUS-RFD analysis have been described previously.[8-13] Briefly, the IVUS-RFD analysis was performed with a dedicated IVUS-VH console (Volcano Therapeutics, Rancho Cordova, CA, USA) during routine coronary angiography after intracoronary administration of 100 to 200 µg of nitroglycerine. A 20-MHz, 2.9 Fr monorail, electronic Eagle Eye Gold IVUS catheter (Volcano Therapeutics) was advanced into the distal to the index sites, and automatic pullback at 0.5 mm/s was done to an proximal to the index sites. The IVUS-RFD image was recorded on a DVD-ROM for offline analysis later.

Spectral analysis of IVUS RFD

Quantitative off line measurements for all the data of global VH registry were done with personal computer VH program software (Volcano Therapeutics) by examiners (Cardialysis BV, Rotterdam, The Netherlands) who were unaware of the clinical characteristics of the subjects. For both the lumen and the media-adventitia interface, semi-automatic contour detection was done for all the frames of the examined coronary segments. Then, the borders were manually corrected in all the frames.[10-12] The lumen and the media-adventitia interfaces at the coronary segments with visible side branch take-off were drew by imaginary lines with the use of longitudinal cross-sectional views to reduce the variability of measurements. For each frame, compositional tissue characteristics were expressed in colours, as previously described (green for fibrous tissue, green-yellow for fibro-fatty, white for dense calcium, and red for necrotic core area).[8] An examiner (SH Han, Mayo clinic, Rochester, MN, USA), blinded to the clinical characteristics of the patients, identified the major coronary bifurcation sites which met the inclusion and exclusion criteria for this study. The proximal and distal segments of bifurcation sites were defined to 5 mm segments proximal and distal to the bifurcation sites with side branch take-off. The segments with side branch take-off were defined to at the bifurcation segments. All cross-sectional frames corresponding to proximal, distal and at the bifurcation segments were analysed and all geometric and compositional parameters were averaged by the numbers of frame counts (Figure 1).

The mean vessel cross-sectional area (CSA), lumen CSA, P+M CSA, P+M burden were calculated. P+M CSA was defined as (vessel CSA - lumen CSA). The P+M burden percent (%) was calculated as: (P+M CSA/vessel CSA) ×100. In addition, compositional parameters such as dense calcium (DC) CSA (reported in square millimetres [mm^2]) and %, fibrous tissue (FT) CSA (mm^2) and %, fibro-fatty

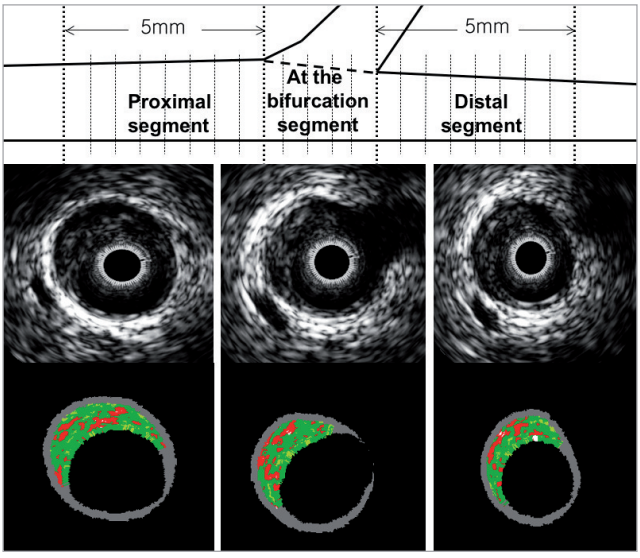

Figure 1. The schematic depiction of proximal, at the bifurcation (the point of the bifurcation), and distal segments of bifurcations (upper panel). Gray intravascular ultrasound (IVUS) (middle panel) and virtual histology (VH)-IVUS (lower panel) of each VH frame were analysed. The numbers of frames corresponding to 5 mm proximal and distal to the bifurcation sites were analysed. At the bifurcation segment the numbers of frames were analysed for each segment length because the numbers of frames at the bifurcation segment depends on the vessel size of branch vessel.

(FF) CSA (mm^2) and %, necrotic core (NC) CSA (mm^2) and % were calculated. The percentage of each compositional parameter was calculated as: [(CSA of each compositional parameter/P+M CSA) ×100]. The intraobserver and interobserver variability of geometric and compositional parameters of IVUS RFD analysis demonstrated acceptable reproducibilities by our groups.[13]

Statistical analysis

Discrete variables are presented as counts and percentages. Continuous variables were summarised as mean±SD. The Pearson χ^2 or Fisher exact test, Student *t* test, and Wilcoxon rank-sum tests were performed, as indicated. The one-way repeated measures analysis of variance was used to compare the geometric and compositional characteristics of plaque for the proximal, at the bifurcation, and the distal segments of bifurcation sites. The Mauchly test of sphericity also was done. If the sphericity assumption was not met, the sphericity assumption was corrected by Greenhouse-Geisser method. *Post hoc* tests were performed by multiple comparisons for the means of all paired combinations of the three repeated measures condition, which were adjusted using the Bonferroni method. Statistical significance was accepted as *p* less than 0.05.

Results

Baseline characteristics of subjects

The IVUS RFD analysis of total 955 subjects enrolled to global VH registry was analysed. The data of IVUS RFD analysis in the sites underwent previous percutaneous coronary intervention within 10 mm of major bifurcations (N=264), in saphenous vein graft, diagonal branch, obtuse marginal branch (N=22), the sites with small bifurcation or no bifurcation site (N=204), the sites with another intervening major side branch (N=110), the sites with inadequate data analysis due to poor image quality or heavy calcified sites (N=52) and the sites with inadequate data analysis due to inadequate length of bifurcation segment (N=64) were excluded from the study. Further, two left main-left circumflex bifurcation sites were excluded from the final analysis due to the very small number.

Finally, 237 subjects, 256 major bifurcation sites (left main (LM) and left anterior descending artery (LAD)=41, LAD and diagonal artery=128, left circumflex artery (LCX) and obtuse marginal artery (OM)=34, right coronary artery (RCA) and acute marginal artery (AM)=53) were analysed. Two different major bifurcation sites were evaluated in 19 subjects.

The baseline characteristics of the study subjects are shown in Table 1. The subjects' mean age was 61.0±11.3 years and 77.2% of subjects were male. The study subjects were presented as stable angina in 145 subjects (61.2%) and acute coronary syndrome in 92 (38.8%). Thirty-five (14.8%) bifurcation lesions (P+M burden > 75%) were included in this study.

Table 1. Baseline characteristics of the study subjects (N=237) and bifurcation sites (N=256).

Variable	Value
Age, years	61.0±11.3
Male	183 (77.2)
Diabetes	49 (20.7)
Hypertension	142 (59.9)
Smoking	
Never	110 (46.4)
Ex	55 (23.2)
Current	72 (30.4)
Clinical presentation	
Stable angina	145 (61.2)
Acute coronary syndrome	92 (38.8)
Total cholesterol, mg/dL	182.9±46.6
Triglycerides, mg/dL	91.0±89.0
HDL-cholesterol, mg/dL	47.5±15.4
LDL-cholesterol, mg/dL	108.7±38.0
Bifurcation site	
LM-LAD	41 (16.0)
LAD-diagonal	128 (50.0)
LCX-OM	34 (13.3)
RCA-AM	53 (20.7)
Bifurcation lesion	
(P+M burden >75%)	35 (14.8)

Data are expressed as number (%) or mean±SD. HDL: high density lipoprotein; LDL: low density lipoprotein; LM: left main coronary artery; LAD: left anterior descending artery; LCX: left circumflex artery; OM: obtuse marginal artery; RCA: right coronary artery; AM: acute marginal artery; P+M: plaque plus media

The baseline characterisation of LM and non-LM bifurcations

Eight subjects were evaluated in both LM-LAD and non-LM bifurcation sites. The subjects with LM-LAD bifurcation sites had a tendency to have diabetes (p=0.08) and a significantly high proportion were taking beta-blockers (p=0.03). The other baseline characteristics of subjects with LM-LAD bifurcation sites (N=41) and non-LM bifurcation sites (N=204) were not significantly different between two groups.

The geometric and compositional characteristics of LM-LAD and non-LM bifurcation sites

Tables 2 and 3 show the geometric and compositional characteristics of proximal, at the bifurcation, and distal segments of LM-LAD and non-LM bifurcation sites. The P+M burden was larger in the distal segments of LM-LAD bifurcation sites than in the proximal and at the bifurcation segments (Table 2, Figure 2A). The % NC and % DC at the bifurcation and distal segments of LM-LAD bifurcation sites was significantly greater than in the proximal segments (Table 2, Figures 2B, C). In contrast, P+M burden, % NC and % DC in the proximal segments of non-LM bifurcation sites was significantly greater than at the bifurcation and distal segments (Table 3, Figures 2A, B, C). Among non-LM bifurcation sites, P+M burden of the proximal segments at the LAD-diagonal and RCA-AM bifurcation sites were significantly larger than those of at the bifurcation or distal segments (Figure 2A). Of interest, % NC of proximal segments at the LAD-diagonal, LCX-OM, and RCA-AM bifurcation sites were significantly greater than those of at the bifurcation or distal segments (Figure 2B). However, % DC was only greater in the proximal segments at the RCA-AM bifurcation sites than those of at the bifurcation and distal segments (Figure 2C).

Table 2. Geometric and compositional characteristics in LM-LAD bifurcation sites (n=41).

Variable	Proximal	At the bifurcation	Distal	ANOVA	P/B	P/D	B/D
Geometrical parameters							
Vessel CSA, mm^2	26.83±5.44	25.65±6.44	18.51±4.30	<0.001	NS	<0.001	<0.001
Lumen CSA, mm^2	16.05±4.55	15.37±5.73	9.85±3.03	<0.001	NS	<0.001	<0.001
P+M CSA, mm^2	10.78±3.64	10.28±3.00	8.66±3.20	<0.001	NS	<0.001	<0.001
P+M burden, %	40.40±11.76	41.15±11.01	46.55±12.08	<0.001	NS	0.002	0.001
Compositional parameters							
DC CSA, mm^2	0.22±0.26	0.37±0.36	0.36±0.36	0.007	0.004	0.076	NS
DC, %	1.89±2.10	3.31±2.87	3.73±3.28	<0.001	<0.001	0.002	NS
FT CSA, mm^2	3.52±2.18	3.43±1.63	2.71±1.78	0.006	NS	0.023	0.003
FT, %	29.88±10.66	31.81±8.87	28.58±10.91	NS			
FF CSA, mm^2	0.89±0.80	1.07±0.81	0.64±0.58	<0.001	0.055	0.003	<0.001
FF, %	13.81±8.66	14.60±7.87	9.94±6.83	<0.001	NS	0.004	<0.001
NC CSA, mm^2	0.61±0.77	0.76±0.70	0.70±0.64	NS			
NC, %	4.89±4.78	6.75±5.09	7.36±6.01	0.006	0.001	0.026	NS
Media CSA, mm^2	4.80±0.53	4.14±0.57	3.91±0.55	<0.001	<0.001	<0.001	0.009
Media, %	49.54±17.02	43.53±13.85	50.38±17.96	0.004	0.003	NS	<0.001

Data are expressed as mean±SD. LM: left main coronary artery; LAD: left anterior descending artery; ANOVA: analysis of variance; CSA: cross-sectional area; P/B: proximal segment vs. at the bifurcation segment; P/D: proximal segment vs. distal segment; B/D: at the bifurcation segment vs. distal segment; P+M: plaque plus media; DC: dense calcium; FT: fibrous tissue; FF: fibro-fatty; NC: necrotic core; NS: not significant.

Table 3. Geometric and compositional characteristics in non-LM bifurcation sites (n=215).

Variable	Proximal	At the bifurcation	Distal	ANOVA	P/B	P/D	B/D
Geometrical parameters							
Vessel CSA, mm^2	17.82±4.68	17.85±4.63	13.75±4.05	<0.001	NS	<0.001	<0.001
Lumen CSA, mm^2	9.12±3.65	9.86±3.72	7.31±2.70	<0.001	<0.001	<0.001	<0.001
P+M CSA, mm^2	8.71±2.89	7.99±2.64	6.44±2.42	<0.001	<0.001	<0.001	<0.001
P+M burden, %	49.41±12.12	45.34±11.21	46.80±10.68	<0.001	<0.001	0.009	NS
Compositional parameters							
DC CSA, mm^2	0.42±0.46	0.30±0.34	0.25±0.29	<0.001	<0.001	<0.001	NS
DC, %	4.57±4.67	3.38±3.44	3.55±3.74	<0.001	<0.001	0.006	NS
FT CSA, mm^2	2.91±1.73	2.61±1.47	1.89±1.30	<0.001	0.004	<0.001	<0.001
FT, %	31.07±10.20	30.46±9.74	26.25±10.94	<0.001	NS	<0.001	<0.001
FF CSA, mm^2	0.91±0.78	1.03±0.85	0.65±0.64	<0.001	0.029	<0.001	<0.001
FF, %	9.83±6.93	12.02±7.44	8.22±6.47	<0.001	<0.001	<0.001	<0.001
NC CSA, mm^2	0.77±0.74	0.57±0.55	0.45±0.45	<0.001	<0.001	<0.001	0.002
NC, %	8.08±6.21	6.47±5.11	6.28±5.05	<0.001	<0.001	<0.001	NS
Media CSA, mm^2	3.70±0.52	3.49±0.46	3.25±0.59	<0.001	<0.001	<0.001	<0.001
Media, %	46.45±14.60	47.68±14.38	55.70±17.00	<0.001	NS	<0.001	<0.001

Data are expressed as mean±SD. LM: left main coronary artery; ANOVA: analysis of variance; CSA: cross-sectional area; P/B: proximal segment vs. at the bifurcation segment; P/D: proximal segment vs. distal segment; B/D: at the bifurcation segment vs distal segment; P+M: plaque plus media; DC: dense calcium; FT: fibrous tissue; FF: fibro-fatty; NC: necrotic core; NS: not significant.

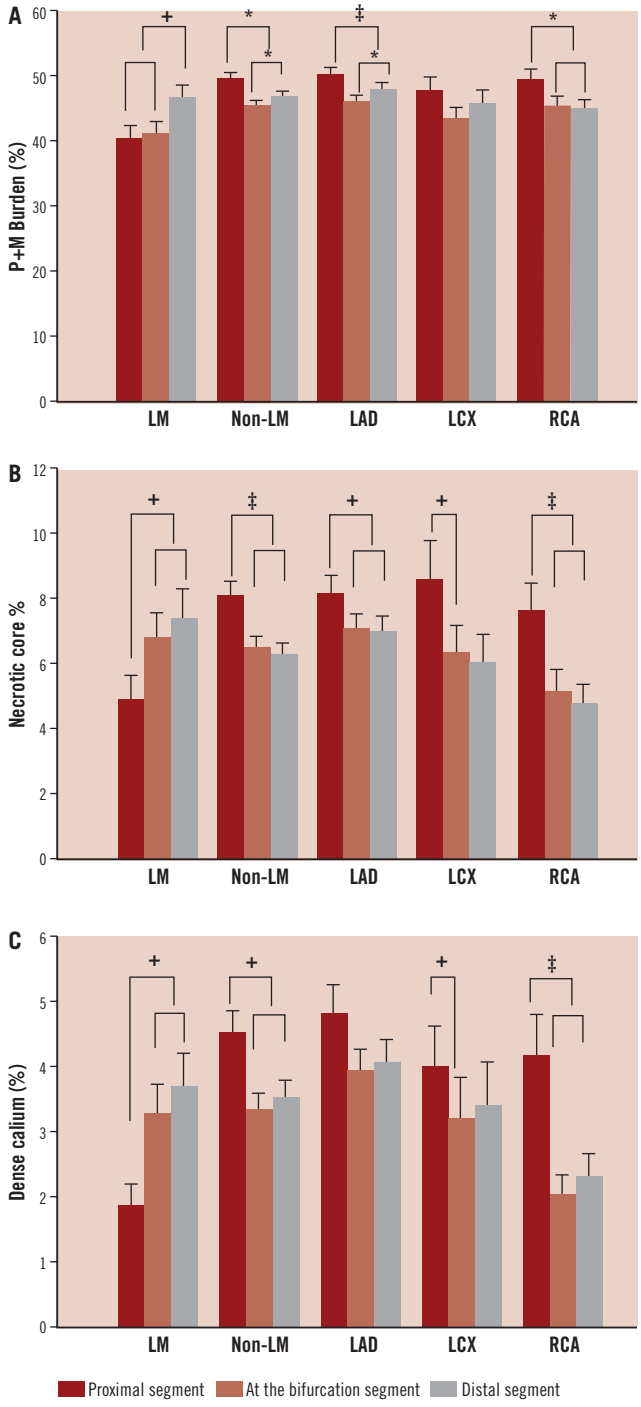

*Figure 2 A. The comparison of plaque+media burden (%) among the proximal, at the bifurcation, and distal segments of left main-left anterior descend artery, non-left main bifurcations. B. The comparison of percent necrotic core among the proximal, at the bifurcation, and distal segments of left main-left anterior descend artery, non-left main bifurcations. C. The comparison of percent dense calcium among the proximal, at the bifurcation, and distal segments of left main-left anterior descend artery, non-left main bifurcations. Values are mean±SEM. LM-LAD: left main-left anterior descend artery; non-LM: non-left main; LAD-D: left anterior descending artery-diagonal; LCX-OM: left circumflex artery-obtuse marginal artery; RCA-AM: right coronary artery-acute marginal artery; *P<0.05, +P<0.01, ‡P<0.001.*

The comparative analysis of compositional characteristics between LM-LAD and non-LM bifurcation sites

Table 4 shows the comparison of compositional characteristics between LM-LAD and non-LM bifurcation sites. The non-LM bifurcation sites had a significantly greater proportion of dense calcium and necrotic core compared with those of the LM-LAD bifurcation sites in the proximal segments of bifurcation sites (all p<0.001).

Table 4. The comparison of compositional characteristics between LM-LAD and non-LM bifurcation sites.

Segment	LM-LAD bifurcation (n=41)	Non-LM bifurcation (n=215)	p Value
Proximal			
DC, %	1.89±2.10	4.57±4.67	<0.001
FT, %	29.88±10.66	31.07±10.20	0.50
FF, %	13.81±8.67	9.83±6.93	0.008
NC, %	4.89±4.78	8.08±6.20	<0.001
Media, %	49.54±17.02	46.45±14.60	0.23
At the bifurcation			
DC, %	3.31±2.87	3.38±3.44	0.90
FT, %	31.81±8.87	30.46±9.74	0.41
FF, %	14.60±7.87	12.02±7.44	0.045
NC, %	6.75±5.09	6.47±5.11	0.75
Media, %	43.53±13.85	47.68±14.38	0.90
Distal			
DC, %	3.73±3.28	3.55±3.74	0.78
FT, %	28.58±10.91	26.25±10.94	0.21
FF, %	9.94±6.83	8.22±6.47	0.12
NC, %	7.36±6.01	6.28±5.05	0.22
Media, %	50.38±17.96	55.70±17.00	0.70

Data are expressed as mean±SD. LM: left main artery; LAD: left anterior descending artery; DC: dense calcium; FT: fibrous tissue; FF: fibro-fatty; NC: necrotic core

Discussion

The current study demonstrates the geometric and compositional characteristics of coronary atherosclerotic plaques at bifurcations sites in humans and shows that LM-LAD bifurcation sites have greater necrotic core and dense calcium at the bifurcation and distal segments of the bifurcation sites compared to proximal segments. In contrast, bifurcation sites of non-LM coronary arteries showed greater necrotic core in the proximal segments. Second, among the non-LM bifurcation sites, the % necrotic core of proximal segments at the LAD-diagonal, LCX-OM, and RCA-AM bifurcation sites were significantly greater than those of at the bifurcation or distal segments. However, dense calcium was only greater in the proximal segments at the RCA-AM bifurcation sites than those of at the bifurcation and distal segments. These results might be attributed to different anatomic locations and other factors such as shear stress and the vessel structure of the bifurcation sites. The current study suggests that there is a heterogeneous, non-uniform distribution of atherosclerotic plaques between LM-LAD and non-LM bifurcation sites.

It is well known that vulnerable plaques and ruptured or prone-to-rupture plaques are non-uniformly distributed along the coronary arteries.[10,14-17] However, little is known about *in vivo* data describing the compositional tissue characteristics of atherosclerosis in the coronary bifurcations on the basis of their anatomic locations. Thus, the current study may have implications on the imaging-guided approach for the detection of the heterogeneous distribution of vulnerable plaque at the complex coronary lesions such as bifurcation sites as well as its potential therapeutic approach for coronary artery disease.

Left main-LAD bifurcations

Previous histologic and IVUS studies of the LM coronary artery bifurcation have demonstrated that atherosclerotic plaques are localised exclusively on the non-flow-dividing walls (opposite to carina) of the LAD and LCX.[4,6,18] Valgimigli et al[19] recently reported that the amount of necrotic core was minimal in left main stem but peaked in the first 6 mm coronary segment from the carina of LM bifurcations and then progressively decreased distally by IVUS-VH study. In addition, Rodriguez-Granillo et al[20] reported that ostial LAD atherosclerotic plaques present larger plaque burden, eccentricity, and plaque thickness than distal LM coronary plaques. In this study, a larger calcified and necrotic core content by IVUS-RFD analysis was found distal to the LCX take-off in the ostial LAD.

In the current study, the segments at the bifurcation and distal to the bifurcations of the LM-LAD had greater % necrotic core and dense calcium compared with the proximal segments. In addition, the P+M burden of the distal segment in the LM-LAD bifurcations was significantly greater than those of the proximal and at the bifurcation segments. It has been known that the LM has the most elastic tissue of the coronary vessels and the amount of elastic tissue was diminished distally in the coronary tree. These histological properties make LM unique among all coronary arteries in the pathogenesis of atherosclerosis.[21,22] These factors may explain the differential tissue characteristics between LM-LAD and non-LM bifurcations. Our study extends previous observations and demonstrates the differential distribution of the component of the plaque in LM-LAD bifurcation sites.

Non-left main bifurcations

Badak et al[23] reported the results of IVUS analysis in the LAD-diagonal and LCX-OM bifurcations. Volumetric analysis showed that vessel CSA, lumen CSA and P+M CSA were larger ($P<0.001$) in the proximal segment than in the distal segment, and the P+M burden was similar between these segments. The data from the current study extends this previous observational study, and reports the tissue characterisation of these sites. Moreover, in the current study we reported that the% necrotic core and dense calcium in the proximal segment of non-LM bifurcations were greater than those of at the bifurcation and distal segments.

In the current study, the % necrotic core in the proximal segments were greater than those of at the bifurcation and distal segments in all non-LM bifurcations. However, the % dense calcium in the proximal segments were greater than those of at the bifurcation and distal segments only in the RCA-AM bifurcation sites. Our results are also consistent with recent published data which showed the proximal segments of bifurcations had been identified as a region more likely to contain thin fibrous cap and a greater proportion of necrotic core.[24]

Clinical implications

A large body of evidence has demonstrated a significant relationship between early atheroma development and low or oscillatory shear forces resulting from vessel bifurcations.[2,20,25-27] Our data suggest that the different anatomic locations and shear forces at the LM-LAD and non-LM bifurcation sites might lead to the formation of atheroma at different sites in proximal, at the bifurcation and distal segments.

Post mortem data suggest also that plaque composition itself plays a pivotal role in determining plaque vulnerability.[28] Our results, which show different geometric and compositional characteristics between LM-LAD bifurcations and non-LM bifurcations, suggest LM-LAD and non-LM bifurcation sites may have a different pattern of plaque rupture.

Bifurcation coronary lesions remain a challenging lesion subset for interventional procedures even in the era of drug-eluting stent.[3] Baseline plaque accumulation has been reported to be related to the long-term outcome of interventional procedures.[29] Nakazawa et al[30] suggested, on the basis of their pathologic data, that lesions with penetration of necrotic core by drug-eluting stent struts may be associated with late stent thrombosis. The importance of characterising the plaque components is underscored by recent studies that have demonstrated that necrotic core-rich lesions assessed by IVUS-RFD analysis were an important predictor of the risk of distal embolisation after stent deployment in patients with myocardial infarction and in patents with elective percutaneous coronary intervention.[31,32]

In the current study, heterogeneous, non-uniform atherosclerotic tissue characteristics were observed in coronary bifurcation sites, and this observation may suggest, at least in part, the less favourable outcome after intervention for bifurcation lesions as compared with the result of intervention for non-bifurcation lesions. Furthermore, our results suggest that more effective interventions such as imaging guided therapeutic approach will be needed for the treatment of lesions at coronary bifurcation sites.

Study limitations

Our study has several limitations. We did not evaluate major bifurcation sites in relation to their anatomic locations in the same subjects. However, the baseline characteristics did not differ between subjects with LM and non-LM bifurcation sites (data are not shown), we believe that there is no bias in enrolling patients to global VH registry in subjects with LM-LAD bifurcation sites and with non-LM bifurcation sites. In addition, we did not evaluate the effects of side branch locations in terms of the orientation of side branch toward the myocardial or epicardial surface and the obliquity of the side branch take-off and did not analyse the characteristics of flow-dividing and non-flow dividing sides of the bifurcation site. Regarding this topic, previous studies using IVUS and multislice computed tomography demonstrated that plaque was more

accumulated in low wall shear stress regions (the opposite wall to the carina, the inner wall of a curved vessel).[23,33] Further study for this topic using IVUS-RFD analysis will be needed in the future. Because most of coronary artery bifurcations enrolled in this study have been shown as mild atherosclerosis, further study to evaluate the tissue characteristics in coronary artery bifurcation lesions, which are indicated to perform coronary interventions, are warranted in the future.

In conclusion, the current study demonstrates that tissue characteristics of plaque differ significantly at coronary bifurcation sites according to their segments (proximal, at the bifurcation, distal segments) and anatomical locations (LM-LAD vs. non-LM bifurcations). These results might be derived from different morphology, anatomic locations (possible angle dependency), and additional factors such as shear stress and vessel structure (elastic vs. muscular) of bifurcation sites. The further investigation for the clinical efficacy of imaging guided therapy on complex coronary plaques such as bifurcation sites are warranted in the future.

References

1. Nerem RM. Vascular fluid mechanics, the arterial wall, and atherosclerosis. *J Biomech Eng.* 1992;114:274-282.

2. Glagov S, Zarins C, Giddens DP, Ku DN. Hemodynamics and atherosclerosis. Insights and perspectives gained from studies of human arteries. *Arch Pathol Lab Med.* 1988;112:1018-1031.

3. Louvard Y, Lefèvre T, Morice MC. Percutaneous coronary intervention for bifurcation coronary disease. *Heart.* 2004;90:713-722.

4. Svindland A. The localization of sudanophilic and fibrous plaques in the main left coronary bifurcation. *Atherosclerosis.* 1983;48:139-145.

5. Grottum P, Svindland A, Walloe L. Localization of atherosclerotic lesions in the bifurcation of the main left coronary artery. *Atherosclerosis.* 1983;47:55-62.

6. Kimura BJ, Russo RJ, Bhargava V, McDaniel MB, Peterson KL, DeMaria AN. Atheroma morphology and distribution in proximal left anterior descending coronary artery: in vivo observations. *J Am Coll Cardiol.* 1996;27:825-831.

7. Nair A, Kuban BD, Obuchowski N, Vince DG. Assessing spectral algorithms to predict atherosclerotic plaque composition with normalized and raw intravascular ultrasound data. *Ultrasound Med Biol.* 2001;27:1319-1331.

8. Nair A, Kuban BD, Tuzcu EM, Schoenhagen P, Nissen SE, Vince DG. Coronary plaque classification with intravascular ultrasound radiofrequency data analysis. *Circulation.* 2002;106:2200-2206.

9. Nair A, Margolis P, Kuban B, Vince D. Automated coronary plaque characterization with intravascular ultrasound backscatter: ex vivo validation. *EuroIntervention* 2007;3:113-120.

10. Rodriguez-Granillo GA, Garcia-Garcia HM, Mc Fadden EP, Valgimigli M, Aoki J, de Feyter P, Serruys PW. In vivo intravascular ultrasound-derived thin-cap fibroatheroma detection using ultrasound radiofrequency data analysis. *J Am Coll Cardiol.* 2005;46:2038-2042.

11. Fujii K, Carlier SG, Mintz GS, Wijns W, Colombo A, Böse D, Erbel R, de Ribamar Costa J Jr, Kimura M, Sano K, Costa RA, Lui J, Stone GW, Moses JW, Leon MB. Association of plaque characterization by intravascular ultrasound virtual histology and arterial remodeling. *Am J Cardiol.* 2005;96:1476-1483.

12. Rodriguez-Granillo GA, Serruys PW, Garcia-Garcia HM, Aoki J, Valgimigli M, van Mieghem CA, McFadden E, de Jaegere PP, de Feyter P. Coronary artery remodeling is related to plaque composition. *Heart.* 2006;92:388-391.

13. Rodriguez-Granillo GA, Vaina S, Garcia-Garcia HM, Valgimigli M, Duckers E, van Geuns RJ, Regar E, van der Giessen WJ, Bressers M, Goedhart D, Morel MA, de Feyter PJ, Serruys PW. Reproducibility of intravascular ultrasound radiofrequency data analysis: implications for the design of longitudinal studies. *Int J Cardiovasc Imaging.* 2006;22:621-631.

14. Shah PK. Mechanisms of plaque vulnerability and rupture. *J Am Coll Cardiol.* 2003;41 Supple S; 15S-22S.

15. von Birgelen C, Klinkhart W, Mintz GS, Papatheodorou A, Herrmann J, Baumgart D, Haude M, Wieneke H, Ge J, Erbel R. Plaque distribution and vascular remodeling of ruptured and nonruptured coronary plaques in the same vessel: an intravascular ultrasound study in vivo. *J Am Coll Cardiol.* 2001;37:1864-1870.

16. Wang JC, Normand SL, Mauri L, Kuntz RE. Coronary artery spatial distribution of acute myocardial infarction occlusions. *Circulation.* 2004;110:278-284.

17. Hong MK, Mintz GS, Lee CW, Lee BK, Yang TH, Kim YH, Song JM, Han KH, Kang DH, Cheong SS, Song JK, Kim JJ, Park SW, Park SJ. The site of plaque rupture in native coronary arteries: a three-vessel intravascular ultrasound analysis. *J Am Coll Cardiol.* 2005;46:261-265.

18. Ding Z, Biggs T, Seed WA, Friedman MH. Influence of the geometry of the left main coronary artery bifurcation on the distribution of sudanophilia in the daughter vessels. *Arterioscler Thromb Vasc Biol.* 1997;17:1356-1360.

19. Valgimigli M, Rodriguez-Granillo GA, Garcia-Garcia HM, Vaina S, De Jaegere P, De Feyter P, Serruys PW. Plaque composition in the left main stem mimics the distal but not the proximal tract of the left coronary artery: influence of clinical presentation, length of the left main trunk, lipid profile, and systemic levels of C-reactive protein. *J Am Coll Cardiol.* 2007;49:23-31.

20. Rodriguez-Granillo GA, Garcia-Garcia HM, Wentzel J, Valgimigli M, Tsuchida K, van der Giessen W, de Jaegere P, Regar E, de Feyter PJ, Serruys PW. Plaque composition and its relationship with acknowledged shear stress patterns in coronary arteries. *J Am Coll Cardiol.* 2006;47:884-885.

21. Bergelson BA, Tommaso CL. Left main coronary artery disease: assessment, diagnosis, and therapy. *Am Heart J.* 1995;129:350-359.

22. El-Menyar AA, Al Suwaidi J, Holmes DR Jr. Left main coronary artery stenosis: state-of-the-art. *Curr Probl Cardiol.* 2007;32:103-93.

23. Badak O, Schoenhagen P, Tsunoda T, Magyar WA, Coughlin J, Kapadia S, Nissen SE, Tuzcu EM. Characteristics of atherosclerotic plaque distribution in coronary artery bifurcations: an intravascular ultrasound analysis. *Coron Artery Dis.* 2003;14:309-316.

24. Gonzalo N, Garcia-Garcia HM, Regar E, Barlis P, Wentzel J, Onuma Y, Ligthart J, Serruys PW. In vivo assessment of high-risk coronary plaques at bifurcations with combined intravascular ultrasound and optical coherence tomography. *JACC Cardiovasc Imaging.* 2009;2:473-482.

25. Zarins CK, Giddens DP, Bharadvaj BK, Sottiurai VS, Mabon RF, Glagov S. Carotid bifurcation atherosclerosis. Quantitative correlation of plaque localization with flow velocity profiles and wall shear stress. *Circ Res.* 1983;53:502-514.

26. Weydahl ES, Moore JE. Dynamic curvature strongly affects wall shear rates in a coronary artery bifurcation model. *J Biomech.* 2001;34:1189-1196.

27. Chatzizisis YS, Coskun AU, Jonas M, Edelman ER, Feldman CL, Stone PH. Role of endothelial shear stress in the natural history of coronary atherosclerosis and vascular remodeling: molecular, cellular, and vascular behavior. *J Am Coll Cardiol.* 2007;49:2379-2393.

28. Virmani R, Kolodgie FD, Burke AP, Farb A, Schwartz SM. Lessons from sudden coronary death: a comprehensive morphological classification scheme for atherosclerotic lesions. *Arterioscler Thromb Vasc Biol.* 2000;20:1262-1275.

29. Hoffmann R, Mintz GS, Mehran R, Pichard AD, Kent KM, Satler LF, Popma JJ, Wu H, Leon MB. Intravascular ultrasound predictors of angiographic restenosis in lesions treated with Palmaz-Schatz stents. *J Am Coll Cardiol.* 1998;31:43-49.

30. Nakazawa G, Finn AV, Virmani R. Vascular pathology of drug-eluting stents. *Herz.* 2007;32:274-280.

31. Kawaguchi R, Oshima S, Jingu M, Tsurugaya H, Toyama T, Hoshizaki H, Taniguchi K. Usefulness of virtual histology intravascular ultrasound to predict distal embolization for ST-segment elevation myocardial infarction. *J Am Coll Cardiol.* 2007;50:1641-1646.

32. Kawamoto T, Okura H, Koyama Y, Toda I, Taguchi H, Tamita K, Yamamuro A, Yoshimura Y, Neishi Y, Toyota E, Yoshida K. The relationship between coronary plaque characteristics and small embolic particles during coronary stent implantation. *J Am Coll Cardiol.* 2007;50:1635-1640.

33. van der Giessen AG, Wentzel JJ, Meijboom WB, Mollet NR, van der Steen AF, van de Vosse FN, de Feyter PJ, Gijsen FJ. Plaque and shear stress distribution in human coronary bifurcations: a multislice computed tomography study. *EuroIntervention.* 2009;4:654-661.